



ChemComm

**Photochemical generation and reactivity of a new  
phthalocyanine-manganese-oxo intermediate**

Journal:	<i>ChemComm</i>
Manuscript ID	CC-COM-03-2023-001275.R2
Article Type:	Communication

SCHOLARONE™  
Manuscripts

## COMMUNICATION

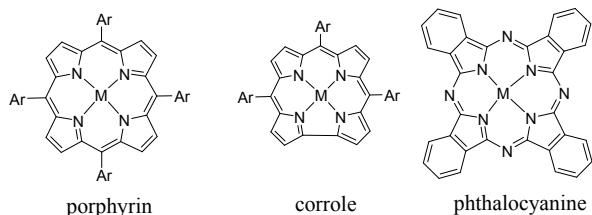
## Photochemical generation and reactivity of a new phthalocyanine-manganese-oxo intermediate

Tristan Skipworth,<sup>a</sup> Seth Klaine,<sup>a</sup> and Rui Zhang\*<sup>a</sup>Received 00th January 20xx,  
Accepted 00th January 20xx

DOI: 10.1039/x0xx00000x

**The first phthalocyanine-manganese-oxo intermediate was successfully generated by visible-light photolysis of chlorate or nitrite manganese(III) precursors, and its reactivity towards organic substrates was kinetically probed and compared with other related porphyrin-metal-oxo intermediates.**

The ubiquitous cytochrome P-450 enzymes (P450s) found in nature with an iron porphyrin core serves as an inspiration for the pursuit of efficient and controllable oxidation catalysis.<sup>1-4</sup> To this end, many synthetic metal complexes such as metalloporphyrins and metalocorroles have been largely synthesized as enzyme-like catalysts for a wide range of catalytic transformations.<sup>5-11</sup> In turn, non-natural metal phthalocyanine complexes (MPC's) are highly desirable not only because of their structural resemblance to heme-containing macrocycles (Scheme 1), but also due to their exceptional redox, optical properties, and ease of straightforward synthesis on a large scale.<sup>12</sup> Thus, MPC's and their binuclear complexes have been found extensive applications as redox catalysts<sup>13-17</sup> including the industrial Merox process.<sup>18</sup>



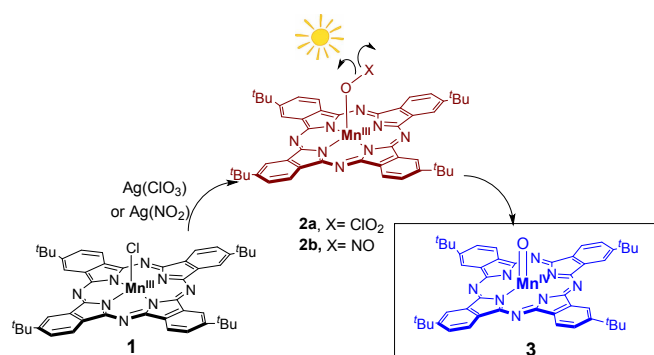
**Scheme 1.** Structures of metal porphyrin, corrole and phthalocyanine

<sup>a</sup> Department of Chemistry, Western Kentucky University, 1906 College Heights Blvd., Bowling Green, Kentucky, USA. Fax: 1-270-7455631; Tel: +1-270-7453803; E-mail: [rui.zhang@wku.edu](mailto:rui.zhang@wku.edu)†

Electronic Supplementary Information (ESI) available: [Experimental details, UV-vis spectra of **2a** and **2b**, time-resolved spectra for generation of **3** from nitrite precursor, and time-resolved spectra for reaction of **3** with triethylamine, and GC traces for preparative oxidations]. See DOI: 10.1039/b000000x/. See DOI: 10.1039/x0xx00000x

In enzymatic and synthetic catalysis, a high-valent transition metal-oxo intermediate is typically formed as the reactive oxygen atom transfer (OAT) species.<sup>19-22</sup> In this context, extensive efforts have been directed to metalloporphyrin as P450s models, and a variety of active metal-oxo species were produced and characterized to elucidate the oxidation mechanisms.<sup>19, 23, 24</sup> In striking contrast, the mechanistic aspects of MPC's catalytic oxidation are still less explored, especially the identification and characterization of the active metal-oxo species.<sup>25</sup> To date, only one high-valent iron(IV)-oxo radical cation species on the phthalocyanine platforms has been detected and spectroscopically characterized.<sup>26</sup> The formation of a diiron-oxo species was also evidenced in  $\mu$ -nitrido *bis*-phthalocyanines.<sup>27</sup> These findings suggest that mechanistic features of MPC-mediated oxidations can be similar to those mediated by their porphyrinoid analogs. Nevertheless, the reactivity of metal-oxo species containing phthalocyanines has never been reported.

To generate and study highly reactive metal-oxo intermediates, photochemical reactions are intrinsically advantageous because activation is achieved by the absorption of a photon, which leaves no residue. On the contrary, most chemical methods rely on the use of toxic or polluting reagents. In this regard, our previously published works<sup>28, 29</sup> have demonstrated that the photochemical production of high-valent transition metal-oxo derivatives is a promising approach with general synthetic utility. As a result, various transition metal-oxo intermediates containing different metals on macrocyclic systems, such as porphyrin,<sup>30-34</sup> corrole<sup>35, 36</sup> and salen ligands<sup>37</sup> have been successfully produced and studied in real time. In this work, we report the application of the photochemical approach using visible light to generate and study a reactive Pc-metal-oxo intermediate that is currently identified as the manganese(IV)-oxo species. Following its generation, the reactivity of this new manganese-oxo species was kinetically probed with organic substrates, including alkenes, benzylic hydrocarbons and alcohols, and sulfides. To the best of our knowledge, this work presents the first photochemical generation and reactivity study of metal-oxo species on the phthalocyanine platform that can be directly compared with the related porphyrin-metal-oxo species.



**Scheme 2.** Visible light generation of a phthalocyanine-manganese-oxo species

In  $\text{CH}_3\text{CN}$ , the readily soluble tetra-*tert*-butylphthalocyanine manganese(III) chloride, denoted as  $\text{Mn}^{\text{III}}(\text{tBu}_4\text{-Pc})\text{Cl}$  (**1**), was treated with 2 equivalents of  $\text{Ag}(\text{ClO}_3)$  or  $\text{Ag}(\text{NO}_2)$  to form the corresponding  $\text{Mn}^{\text{III}}(\text{Pc}^t\text{Bu}_4)(\text{ClO}_3)$  (**2a**) or  $\text{Mn}^{\text{III}}(\text{Pc}^t\text{Bu}_4)(\text{NO}_2)$  (**2b**) (Scheme 2), and their formation was indicated by UV-vis spectroscopy (Fig. S1 in ESI). Compounds **2** are highly photo-labile, and subsequent irradiation of **2a** in  $\text{CH}_3\text{CN}$  with visible light (120W from a SOLA light engine Lumencor) produced an *ocean-blue* transient **3** with the characteristic absorbances at 620 (Q-band) and 325 nm (Soret-band). Figure 1 shows the time-resolved spectra for the photochemical transformation of **2** to **3** over a period of 40 s with clean isosbestic points at 775, 656, 454, and 336 nm. The distinct blue-shift observed in the Q-band of species **3** is suggestive of redox transformation occurring on the metal center instead of the ligand, because the ligand-based transformations typically result in a collapse of the Q-band and formation of a broad band at around 500 nm.<sup>38</sup> The same species **3** apparently was also formed from nitrite **2b** upon irradiation, albeit with slightly reduced efficiency compared to **2a** (see Fig. S2 in ESI). Under identical conditions, however, continuous photolysis of manganese(III) phthalocyanines containing chloride, perchlorate, or nitrate did not result in any noticeable reactions. Control experiments showed that no species **3** was formed in the absence of light. Moreover, the generation of **3** was found to be slower when the power of the irradiating light decreased (see Inset of Figure 1). It should be noted that attempts to produce the manganese-oxo **3** at a higher concentration ( $> 10^{-4}$  M) were not successful due to the total blockage of the visible light, resulting in inert photochemical reactions.

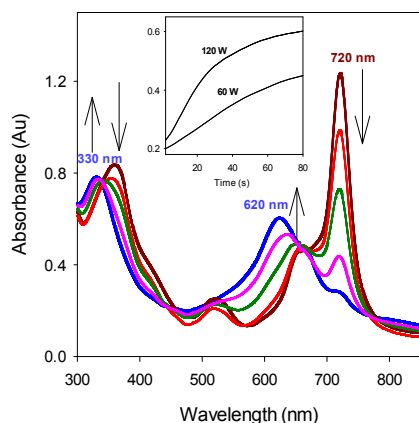


**Fig. 1.** Time-resolved spectra of **3** following irradiation of **2a** ( $2 \times 10^{-5}$  M) with visible light (120 W) in  $\text{CH}_3\text{CN}$  solution at 23 °C over 40 s.

Inset is kinetic traces monitored at 620 nm with different power of irradiating lights.

The photo-generated species **3** was characterized by electron spray ionization mass spectrometry (ESI MS) that we recently used to detect high-valent manganese(IV)-oxo porphyrins<sup>39</sup> and chromium(IV)/(V)-oxo porphyrins.<sup>40</sup> As shown in Figure 2, the ESI-MS spectrum exhibited a moderate cluster at  $m/z = 808.3$  that perfectly matches the calculated  $M+1$  of  $[\text{Mn}(\text{tBu}_4\text{-Pc})(\text{O})]$ , along with a strong peak at  $m/z = 791.3$  assigned to the stable ionic fragment of  $[\text{Mn}(\text{tBu}_4\text{-Pc})]^+$ . Of note, the simulated isotope distribution pattern for  $[\text{Mn}(\text{tBu}_4\text{-Pc})(\text{O})]$  obtained through calculation was found to be in agreement with the observed pattern (see inset of Figure 2A). Importantly, when a small amount of  $\text{H}_2^{18}\text{O}$  was added to the sample of **3** and incubated for 2 min, the ESI MS spectrum (Figure 2B) revealed that the molecular peak of  $m/z$  808, i.e.  $[\text{Mn}(\text{tBu}_4\text{-Pc})(^{16}\text{O})]$ , partially shifted to  $m/z$  810 (approximate 55%), which corresponds to  $^{18}\text{O}$ -substituted  $[\text{Mn}(\text{tBu}_4\text{-Pc})(^{18}\text{O})]$ . This observation is in accordance with the expected behavior of high-valent metal-oxo species, wherein the oxo ligand exchanges with  $^{18}\text{O}$ -labelled  $\text{H}_2^{18}\text{O}$ .<sup>41</sup>

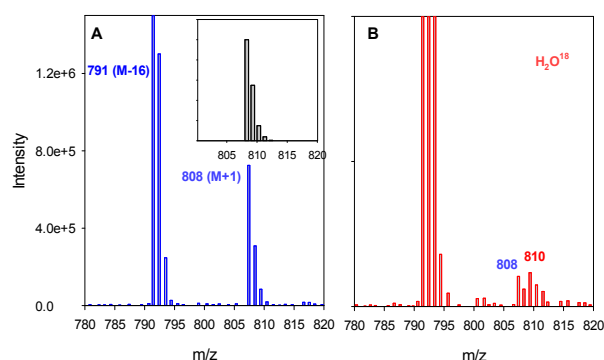


**Fig. 2.** (A) ESI-MS spectrum in a positive mode of **3** ( $2 \times 10^{-5}$  M) in  $\text{CH}_3\text{CN}$ . Inset showing the simulated isotope distribution pattern for  $[\text{Mn}(\text{tBu}_4\text{-Pc})(\text{O})]$ ; (B) ESI-MS spectrum of  $^{18}\text{O}$ -labelled **3** after 2 min incubation with 15  $\mu\text{L}$   $\text{H}_2^{18}\text{O}$  per 1 mL of  $2 \times 10^{-5}$  M solution.

The preparative reaction with an alkene substrate confirmed that transient **3** is a reactive OAT species. Chlorate precursor **2a** (10  $\mu\text{mol}$ ) was prepared by mixing **1** with 2 equiv. of  $\text{Ag}(\text{CO}_3)$  in  $\text{CH}_3\text{CN}$  (20 mL); under visible light irradiation for 5 min, the yield of **3** determined by UV-visible spectroscopy was  $> 95\%$ . An excess of *cis*-cyclooctene was added, and after 30 min, the mixture was analyzed by quantitative GC-MS, which showed the presence of *cis*-cyclooctene oxide in 92% yield based on precursor **2a**. In a similar fashion, stoichiometric oxidations of other organic substrates were conducted, and the resulting oxidized products and their corresponding yields were determined and documented in Table 1, and corresponding GC traces are in ESI.

**Table 1.** Stoichiometric oxidations of organic substrates by **3**<sup>a</sup>

substrate	oxidized products (yield%) <sup>b</sup>
<i>cis</i> -cyclooctene	<i>cis</i> -cyclooctene oxide (92%)
cyclohexene	cyclohexene oxide (12%), 2-cyclohexenol (9%), 2-cyclohexenone (37%)
styrene	styrene oxide (30%), benzaldehyde (46%)
ethylbenzene	1-phenylethanol (11%), acetophenone (40%)
1-phenylethanol	acetophenone (94%)
thioanisole	sulfoxide (76%), sulfone (9%)

<sup>a</sup>Reactions for product analysis were carried out in  $\text{CH}_3\text{CN}$  at a higher amount of **3** (ca. 10  $\mu\text{mol}$ ) and a large excess of organic substrates in 20 mL vial and

monitored by UV-vis spectroscopy for completion of the reaction. <sup>b</sup> Oxidized products were identified by GC-MS with an MSD libraries from Agilent. Yields were calculated based on precursor **2a** used for generation of **3** (> 95%) by GC analysis of the spent reaction solutions with internal standard

In this study, each of the reactions of [Mn<sup>IV</sup>(Pc)(O)] with above mentioned substrates appeared to be a two-electron process, despite not detecting the formation of Mn(II) product. Figure 3A shows the representative time-resolved spectra of species **3** reacting with various two-electron reductants such as ethylbenzene. Clean isosbestic points were observed with all substrates in time-resolved spectra, suggesting the conversion of **3** to manganese(III) product does not involve any accumulated intermediates. This spectral observation in Figure 2 A. indicates that oxidation reactions of the transient Mn<sup>II</sup> products resulting from the oxidation of substrate occur at a faster rate than that of the reactions of [Mn<sup>IV</sup>(Pc)(O)] with the substrate, consistent with previous findings with [Mn<sup>IV</sup>(Por)O], where the Mn<sup>III</sup> complex is also formed as the final product in the two-electron process.<sup>39</sup> In kinetic studies, we monitored the absorbance in the Q-band at 620 nm, which decreased over the course of reaction. As shown in Figure 3B, the pseudo-first-order decay rate constants increased linearly with substrate concentration. The kinetic data were solved by eq. 1, where  $k_{\text{obs}}$  is the observed rate constant,  $k_0$  is the background rate constant (near-zero),  $k_{\text{ox}}$  is the second-order rate constant for oxidation of substrate, and [Sub] is the concentration of substrate. The second-order rate constants for **3** are summarized in Table 2. For the purpose of comparison, a limited number of absolute rate constants for reactions by other reactive metal-oxo porphyrins in acetonitrile is also included.

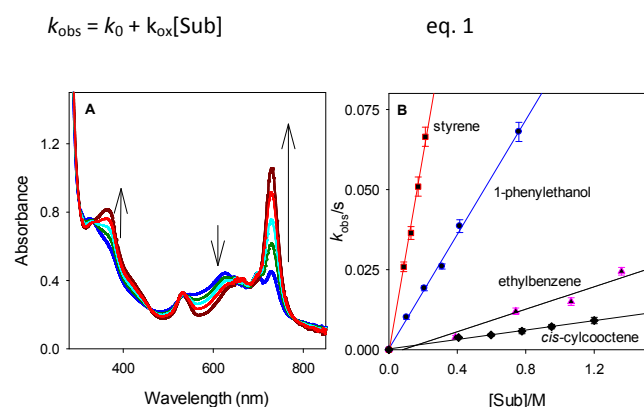


**Fig. 3.** (A) Time-resolved spectra of species **3** reacting in CH<sub>3</sub>CN solution with ethylbenzene (1.2 M) over 100 s at 23 ± 2 °C; (B) Kinetic plots of the observed rate constants for the reaction of **3** versus the concentrations of organic substrates.

In general, the photo-generated species **3** is capable of oxidizing many organic substrates successfully. However, kinetic data in Table 1 revealed that the reactivity of species **3** is modest, with rate constants of  $k_{\text{ox}}$  ranging from  $4.1 \times 10^{-3} \text{ M}^{-1}\text{s}^{-1}$  for *cis*-cyclooctene to  $1.3 \text{ M}^{-1}\text{s}^{-1}$  for thioanisole. When compared with other high-valent metal-oxo species, the reactivity of **3** is similar to that of a neutral manganese(IV)-oxo species containing a highly electron-deficient porphyrin ligand (TPFPP = 5,10,15,20-tetrakis(pentafluorophenyl)porphyrin).<sup>39</sup> In contrast, the related manganese(V)-oxo TPFPP cation produced in our previous studies<sup>30</sup> is considerably more reactive than species **3**. For example, the rate constants for oxidations by TPFPP-manganese(V)-oxo species of styrene and ethylbenzene are at least 6 orders of magnitude larger than those for oxidations by **3**. With the same substrate, iron(IV)-oxo tetramesitylphenylporphyrin (TMP) radical cation,<sup>42</sup> compound **1**

analogue, also reacted more than 3 orders of magnitude faster than species **3**. In addition, a kinetic isotope effect (KIE) was probed using ethylbenzene-*d*<sub>10</sub> as the substrate. However, its oxidation rate is too slow to be precisely determined ( $k_{\text{obs}} < 10^{-4} \text{ s}^{-1}$ , near the range of self-decay rate), indicating a substantial KIE value of > 10. Previously reported studies have shown much smaller KIE values of 2.3<sup>30</sup> for TPFPP-manganese(V)-oxo and 9.9<sup>39</sup> for TPFPP-manganese(IV)-oxo species, respectively.

**Table 2.** Second-order rate constants for oxidations of organic substrates by **3** and other known metal-oxo porphyrins<sup>a</sup>

substrate	<b>3</b> <sup>b</sup>	[Mn <sup>IV</sup> (TPFPP)(O)] <sup>c</sup>	[Mn <sup>V</sup> (TPFPP)(O)] <sup>d</sup>	[Fe <sup>IV</sup> (TMP)(O)] <sup>e</sup>
<i>cis</i> -cyclooctene	(4.1 ± 0.4)E-3	(1.8 ± 0.4)E-2		(6.2 ± 0.2)E1
cyclohexene	(9.4 ± 0.5)E-3			(6.8 ± 0.1)E1
PhCH=CH <sub>2</sub>	(3.1 ± 0.3)E-1		(6.1 ± 0.3)E5	(1.9 ± 0.1)E1
PhCH <sub>2</sub> CH <sub>3</sub>	(1.8 ± 0.5)E-2	(7.1 ± 0.3)E-1	(1.1 ± 0.1)E5	1.6 ± 0.1
PhCH(OH)CH <sub>3</sub>	(8.9 ± 0.2)E-2			
4-F-PhSCH <sub>3</sub>	1.3 ± 0.3	2.0 ± 0.1		

<sup>a</sup> In CH<sub>3</sub>CN at ambient temperature with the units of M<sup>-1</sup>s<sup>-1</sup>; <sup>b</sup> From this work; <sup>c</sup> Data from ref.39; <sup>d</sup> Data from ref.30; <sup>e</sup> Data from ref.42.

In light of its relatively low reactivity that is comparable to that of the related porphyrin-manganese(IV)-oxo intermediates, the structure of **3** was formulated as the Pc-manganese(IV)-oxo species, i.e. [Mn<sup>IV</sup>(<sup>t</sup>Bu<sub>4</sub>-Pc)(O)] shown in Scheme 2. Correspondingly, the photo-generation of [Mn<sup>IV</sup>(<sup>t</sup>Bu<sub>4</sub>-Pc)(O)] is rationalized by *homolytic* cleavage of the O–X (X = Cl or N) bond that resulted in one-electron oxidation of the metal. Although a heterolytic pathway could be possible, but unlikely in this study due to the fact that it would produce much more reactive manganese(V)-oxo species, which is not supported by our reactivity studies. Analogous photo-ligand cleavage reactions involving same homolytic photolysis of corresponding chlorate or nitrite precursors were previously employed to generate [Mn<sup>IV</sup>(Por)(O)],<sup>39</sup> [Mn<sup>V</sup>(corrole)(O)],<sup>35, 36</sup> [Fe<sup>IV</sup>(Por)(O)]<sup>43</sup> and [Cr<sup>IV</sup>(Por)(O)].<sup>37</sup> To further validate the generation of Mn<sup>IV</sup>-oxo species, trimethylamine was used as a one-electron reductant, which rapidly reduced **3** to Mn<sup>III</sup> product without formation of any intermediate (see Fig. S3 in ESI).

In conclusion, we report a photochemical generation and characterization of a novel manganese(IV)-oxo phthalocyanine species. Its reactivity was kinetically probed with different two-electron reductants, allowing for a direct comparison with other high-valent porphyrin-metal-oxo intermediates. The assignment of a manganese(IV)-oxo structure to transient **3**, rather than a manganese(V)-oxo or manganese(IV)-oxo radical cation, is tentative until the species can be produced in higher concentrations that permit more in-depth characterization such as EPR analysis. Nonetheless, the manganese(IV)-oxo formulation is supported by the UV-vis spectrum, the one-electron reduction of **3** to manganese(III) product without intermediate detection, and especially its modest reactivity, as well as the similar photochemical reactions that produced other metal-oxo intermediates. We are currently investigating mechanistic aspects of the photo-generated **3** in oxidation reactions, as well as exploring photo-synthetic methodologies to produce other high-valent metal-oxo phthalocyanines that have not yet been discovered.

We greatly appreciate the National Science Foundation (CHE 2154579) for funding this research. We also thank Dr. Pauline Norris from the Advanced Material Institute at WKU for her assistance with ESI-MS measurements.

Tristan Skipworth: **Investigation, Validation, Visualization**. Seth Klaine: **Investigation, Validation**. Rui Zhang: **Conceptualization, Methodology, Writing – original draft, Supervision, Funding acquisition**.

### Conflicts of interest

There are no conflicts to declare.

### Notes and references

§§ Abbreviations used in this study: Pc = phthalocyanine; MPC's = metal phthalocyanine complexes; Por = porphyrin; TPFPP = 5,10,15,20-tetrakis(pentafluoroporphyrin); TMP = 5,10,15,20-tetramesitylporphyrin; OAT = oxygen atom transfer.

- M. Sono, M. P. Roach, E. D. Coulter and J. H. Dawson, *Chem. Rev.*, 1996, **96**, 2841-2887.
- P. R. Ortiz de Montellano, ed., *Cytochrome P450 Structure, Mechanism, and Biochemistry*, Kluwer Academic/Plenum, New York, 2005.
- I. G. Denisov, T. M. Makris, S. G. Sligar and I. Schlichting, *Chem. Rev.*, 2005, **105**, 2253-2277.
- X. Huang and J. T. Groves, *Chem. Rev.*, 2018, **118**, 2491-2553.
- B. Meunier, *Chem. Rev.*, 1992, **92**, 1411-1456.
- I. Aviv and Z. Gross, *Chem. Commun.*, 2007, 1987-1999.
- C.-M. Che and J.-S. Huang, *Chem. Commun.*, 2009, 3996-4015.
- I. Aviv-Harel and Z. Gross, *Chem. Eur. J.*, 2009, **15**, 8382-8394.
- M. Costas, *Coord. Chem. Rev.*, 2011, **255**, 2912-2932.
- R. A. Baglia, J. P. T. Zaragoza and D. P. Goldberg, *Chem. Rev.*, 2017, **117**, 13320-13352.
- G. Mukherjee, J. K. Satpathy, U. K. Bagha, M. Q. E. Mubarak, C. V. Sastri and S. P. de Visser, *ACS. Catal.*, 2021, **11**, 9761-9797.
- Phthalocyanines: Properties and Applications*, VCH: Weinheim, Germany, 1996.
- B. Meunier and A. B. Sorokin, *Acc. Chem. Res.*, 1997, **30**, 470-476.
- A. B. Sorokin, *Chem. Rev.*, 2013, **113**, 8152-8191.
- P. Afanasiev and A. B. Sorokin, *Acc. Chem. Res.*, 2016, **49**, 583-593.
- A. B. Sorokin, *Coord. Chem. Rev.*, 2019, **389**, 141-160.
- A. B. Sorokin, *Catal. Today*, 2021, **373**, 38-58.
- B. Basu, S. Satpathy and A. K. Bhatnagar, *Catal. Rev.*, 1993, **35**, 571-609.
- B. Meunier, ed., *Metal-Oxo and Metal-Peroxo Species in Catalytic Oxidations*, Springer-Verlag, Berlin, 2000.
- M. Costas, M. P. Mehn, M. P. Jensen and L. Que, *Chem. Rev.*, 2004, **104**, 939-986.
- H. Fujii, *Coord. Chem. Rev.*, 2002, **226**, 51-60.
- D. P. Goldberg, *Acc. Chem. Res.*, 2007, **40**, 626-634.
- J. Rittle and M. T. Green, *Science*, 2010, **330**, 933-937.
- S. P. de Visser and W. Nam, in *Handbook of Porphyrin Science*, eds. K. M. Kadish, K. M. Smith and R. Guilard, World Scientific Publishing, Singapore, 2010, vol. 10, pp. 85-139.
- A. B. Sorokin and E. V. Kudrik, *Catal. Today*, 2011, **113**, 8152-8191.
- P. Afanasiev, E. V. Kudrik, F. Albrieux, V. Briois, O. I. Koifman and A. B. Sorokin, *Chem. Commun.*, 2012, **48**, 6088-6090.
- U. İsci, A. S. Faponle, P. Afanasiev, F. Albrieux, V. Briois, V. Ahsen, F. Dumoulin, A. B. Sorokin and S. P. de Vissor, *Chem. Sci.*, 2015, **6**, 5063-5075.
- R. Zhang and M. Newcomb, *Acc. Chem. Res.*, 2008, **41**, 468-477.
- R. Zhang, S. Klaine, C. Alcantar and F. Bratcher, *J. Inorg. Biochem.*, 2020, **212**, 111246.
- R. Zhang, J. H. Horner and M. Newcomb, *J. Am. Chem. Soc.*, 2005, **127**, 6573-6582.
- Y. Huang, E. Vanover and R. Zhang, *Chem. Commun.*, 2010, **46**, 3776-3778.
- R. Zhang, E. Vanover, W.-L. Luo and M. Newcomb, *Dalton Transactions*, 2014, **43**, 8749-8756.
- T. H. Chen, N. Asiri, K. W. Kwong, J. Malone and R. Zhang, *Chem. Commun.*, 2015, **51**, 9949-9952.
- K. W. Kwong, C. M. Winchester and R. Zhang, *Inorg. Chim. Acta*, 2016, **451**, 202-206.
- K. W. Kwong, N. F. Lee, D. Ranburg, J. Malone and R. Zhang, *J. Inorg. Biochem.*, 2016, **163**, 39-44.
- N. F. Lee, J. Malone, H. Jeddı, K. W. Kwong and R. Zhang, *Inorg. Chem. Commun.*, 2017, **82**, 27-30.
- S. Klaine, N. F. Lee, A. Dames and R. Zhang, *Inorg. Chim. Acta*, 2020, **509**, 119681.
- A. B. P. Lever, E. R. Milaeva and G. Speier, in *Phthalocyanines: Properties and Applications*, eds. C. C. Leznoff and A. B. P. Lever, VCH, New York, 1993, vol. 3, pp. 1-69.
- S. Klaine, F. Bratcher, C. M. Winchester and R. Zhang, *J. Inorg. Biochem.*, 2020, **204**, 110986.
- T. Skipworth, M. Kshahimov, I. Ojo and R. Zhang, *J. Inorg. Biochem.*, 2022, **237**, 112006.
- J. Bernadou and B. Meunier, *Chem. Commun.*, 1998, 2167-2173.
- Z. Pan, R. Zhang and M. Newcomb, *J. Inorg. Biochem.*, 2006, **100**, 524-532.
- N.-F. Lee, D. Patel, H. Y. Liu and R. Zhang, *J. Inorg. Biochem.*, 2018, **183**, 56-65.